New Die to Database Inspection Algorithm for Inspection of 90-nm Node Reticles

Hector Garcia, William Volk, Sterling Watson, Carl Hess; Chris Aquino, Jim Wiley, Chris Mack
(KLA-Tencor, San Jose, CA 95134)

ABSTRACT

The implementation of low k_1 193nm lithography for 90nm node IC production brings new challenges to reticle inspection systems. The inspection tools have to deal with new attenuating films, smaller and more complex features, and more aggressive OPC. In addition, low k_1 lithography causes the mask error factor (MEEF) to increase, magnifying CD errors. This, in turn, makes reticle defect detection specifications more aggressive.

Achieving high sensitivity, low false defect count, for a full plate inspection is a big challenge. Those three (high sensitivity, low false defect count, full plate inspection) are the three "legs" that must support real die-to-database inspection. In order to demonstrate inspection success, all three must be achieved. Without any of them, there is no die-to-database inspection solution. The capabilities described in this paper (the XPE die-to-database algorithm working with the KLA-Tencor TeraStar™ SLF87 system) were developed precisely because no tool in the industry was capable of meeting all of these requirements. The industry was in urgent need of a die-to-database system that is capable of inspecting reticles for the 90nm node at high sensitivity, with a low false defect count for a full plate inspection.

XPE, the new die-to-database inspection algorithm for the TeraStar SLF87 (XPE-87), has been developed for the inspection of 193nm lithography reticles to be used for the 90nm node and beyond. XPE-87 uses new and improved methods for database rendering, defect detection and image contrast adjustment. The algorithm can accommodate the reticle characteristics, inspecting plates with complex features and advanced Sub-Resolution Assist Features (SRAFs) at high sensitivity and low false defect count. Thanks to enhancements to system hardware and light calibration routines, the algorithm is very effective at inspecting 90nm node ArF half-tone reticles.

XPE-87 has been characterized with 193nm and 248nm EPSM versions of Spica, a new programmed defect test reticle. In the presence of complex OPC, results show a substantial improvement in sensitivity compared to previous die-to-database inspection algorithms. The new algorithm has also been used to inspect a variety of 193nmEPSM, 248 EPSM and chrome on glass production reticles. The results show significant improvement for the inspection of 90nm node half-tone reticles including plates with SRAFs.

Simulations were performed to verify the XPE-87 potential for defect detection. Evaluating changes in signal profile due to the presence of defects, a comparison was performed between the aerial profile of the XPE-87 at UV inspection aerial image and the wafer print aerial image at 193nm. The results, show a larger signal for defects in small lines.

Keywords: Reticle, Mask, Inspection, ArF, SRAF, OPC, CD, Defect, Aerial, Database

1. INTRODUCTION

Die-to-die and die-to-database are the two pattern defect reticle inspection methods that are used in the industry. Die-to-die compares one die against another on the same reticle. For this to be possible, both dice must have the same design. The inspection system will scan the areas to be inspected, collecting images and processing them in order to identify differences between dice. Differences that exceed a preset threshold level are detected as defects. Since two or more dice with identical design are needed for die-to-die to work, single die reticles are not inspectable in this mode. That is the main limitation of die-to-die inspection.

Photomask and Next-Generation Lithography Mask Technology X, Hiroyoshi Tanabe, Editor, Proceedings of SPIE Vol. 5130 (2003) © 2003 SPIE · 0277-786X/03/$15.00

Die-to-database inspection is done by comparing images collected from the reticle to images that are rendered from the design data used to write the reticle. In order for this method to be successful, the rendered images must resemble the processed features on the reticle as closely as possible. By its own nature, die-to-database is a more complicated process, requiring advanced algorithms for both data rendering, image processing and defect detection. It also requires more processing power. However, one of the great advantages of die-to-database is the ability to inspect single die reticles and in general, 100% of any reticle layout. Single die reticles are used for many purposes including reticles for development and debugging of new lithography processes and techniques, multi-product shuttle reticles, server chip MPU reticles, etc.

Every new generation of product in the IC industry, brings with itself challenges for die-to-database inspection. Product for the 90nm node is no different. The challenges, described in detail in the next section, present a challenge for die-to-database inspection. The industry was in urgent need of a die-to-database system that is capable of inspecting reticles for the 90nm node at high sensitivity with a low false defect count for a full plate inspection. Before the developments described in this paper, no die-to-database inspection system was capable of meeting all of these requirements.

2. RETICLE INSPECTION CHALLENGES FOR THE 90nm NODE

Reticles for the 90nm node are much more complex than previous ones. They present a series of challenges to the inspection tools that are difficult to overcome. Reticle inspection systems have to deal with new materials, smaller and more complex features, and aggressive OPC. In addition, the implementation of low k_1 lithography on DUV scanners causes the MEEF to increase, magnifying reticle CD errors. This, in turn, makes the reticle defect detection specifications more aggressive. The challenge is particularly difficult for die-to-database inspections.

2.1 ArF High Transmission at Inspection Wavelength

In the past, reticles were made using a thin film containing chromium on quartz substrates, commonly known as Chrome on Glass (COG). In general, the chrome film is very opaque, which means not much light is transmitted thorough it. Because of that, there will be high illumination contrast between clear (quartz) and opaque areas (Chrome). High contrast helps the inspection tool to achieve a high signal to noise ratio, the key to achieving high sensitivity with low false defect count.

As the industry evolved, “half-tone” Embedded Attenuated Phase Shift Masks (EPSMs) became more common. EPSMs are now used with 365nm I-line, 248nm KrF and 193nm ArF lithography. EPSM reticles are made using a thin film of Molybdenum Silicide (MoSi). This material allow for an engineered 180 degree shift in the phase of the exposure light at the wafer plane, affording enhanced contrast at the edges of a line or feature. Being more transmissive than COG at inspection wavelength, MoSi EPSM reticles raised the level of difficulty for inspection. Fig. 1 shows a generic transmission curve for typical ArF and KrF EPSM materials. The curve for KrF lithography EPSM film, shows that transmissivity is approximately 6% at 248nm and 20% at 363.8nm (the UV wavelength used by KLA-Tencor’s TeraStar SLF series). As compared with COG, clearly the KrF lithography material shows less contrast between clear and dark features. After some improvements, the inspection systems were able to get enough contrast for inspection of KrF EPSM reticles. The case for ArF lithography reticles is more severe. The industry has been experimenting with several types of ArF lithography materials. Currently, the most widely used material is 6% transmissive at 193nm. The same material is also approximately 50% transmissive at the UV inspection wavelength. Clearly, given the high transmission at the inspection wavelength, the contrast between clear and dark is reduced significantly. Without enough contrast, high sensitivity, low false, full plate inspection is very difficult.

Expanding this concept, Fig. 2 shows a light profile comparison between an aerial image at 193nm and at the UV inspection wavelength for a clear space. To obtain the profiles, simulations were performed using PROLITH version 7.2.2. The comparison is shown for both space on COG and space on ArF. Clearly, for the COG case, the UV inspection light profile shows a larger contrast between clear and dark than the 193nm one. For the ArF case, at UV inspection wavelength, the opaque region is more transmissive. As a consequence, there is less of a contrast between

clear and dark. Previous inspection tools were unable to compensate for this degree of image contrast. This problem had to be solved in order to achieve high sensitivity.

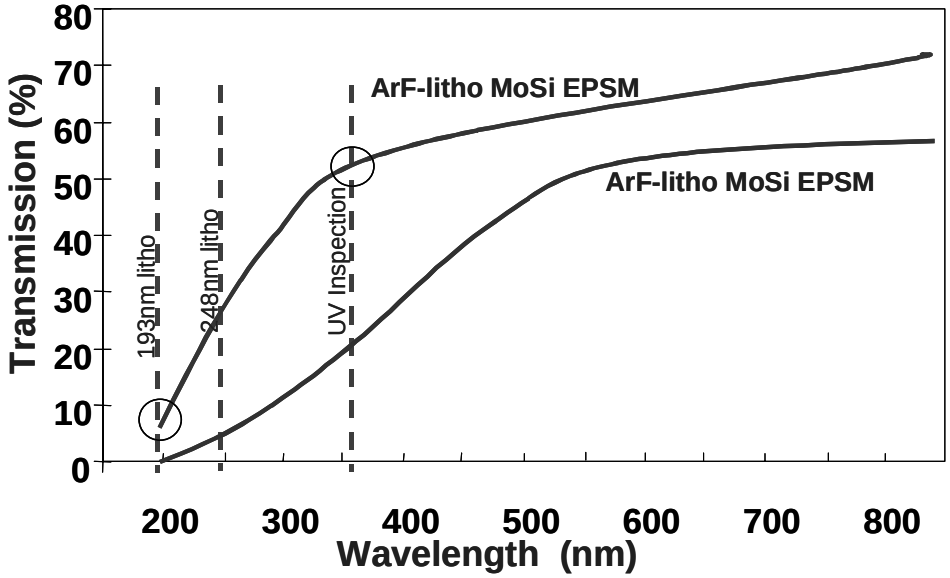

Fig. 1. Optical properties of MoSi shifter used for 248-KrF and 193-ArF

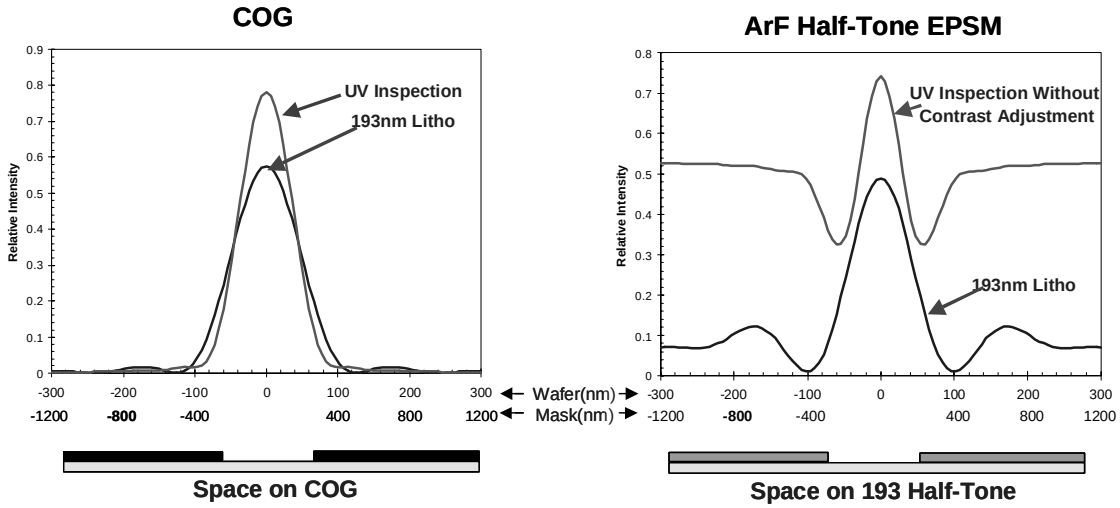

Fig. 2. Aerial Images of a 100nm clear space (400nm on reticle) for COG and ArF EPSM

2.2 Database Image Rendering Problems

Reticle non-linearities are also a problem that needs to be considered for high resolution database inspection. After the manufacturing process, the features on the plate will not look exactly like the corresponding features on the design data. This is due to changes introduced during the manufacturing process, changes that are a characteristic of the process itself (corner rounding, line-width bias and line-end shortening are the prevalent ones). Some changes are

also introduced on purpose (that is the case of bias introduced to reach a target CD). Fig. 3 shows examples of features on reticles with the corresponding design data overlapped on top. The differences between reticle and design data are clear.

A die-to-database inspection compares images collected from the reticle to rendered images that are generated from the design data. During inspection, the inspection station collects images from the plate. These images are compared to corresponding images from the database. To make inspection possible, the reference features are compensated so that they look like the features on the plate. Without this step, all the bias and corner rounding differences between plate and data would be detected as defects. The closer the rendered database images look like the plate the better the chances of inspecting the plate at high sensitivity.

Rendering would be easier if the plate bias and rounding variations were linear. Unfortunately, non-linear variations are common. There are several contributors to reticle non-linearity. The main ones are:

- The exposure step: This is one of the biggest contributors. It depends on the writing tool [(2)], resist, etc.
- Development
- Etching
- Imaging: This is the inspection system contribution

The effect of these contributors to non-linearity is compounded. As a result, a reticle with two-dimensional (2-D) non-linear variations that are complex and consequently difficult to model is produced. Fig. 4 shows an exaggerated artist rendition of the differences between plate and design data. It is common to see miss-matches in line-widths, edge placement, corner rounding, and line-end shortening. Clearly, we can see that no simple rendering model is going to be good enough for high-sensitivity inspection of 90nm node plates because of large residues (the difference between images from the plate and rendered data images) that can be detected as false defects. A new more accurate database 2-D rendering is needed. Without it, high sensitivity inspection is not achievable.

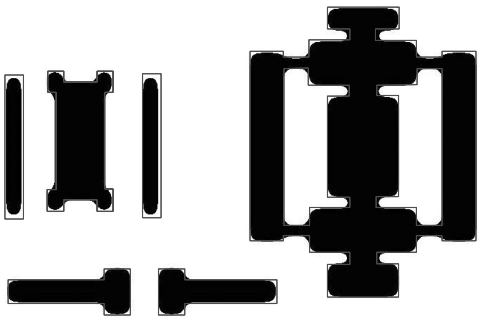

Fig. 3. Samples of reticle features with the corresponding design data overlapped. Differences due to corner rounding, edge bias/placement and line-end shortening are noticeable

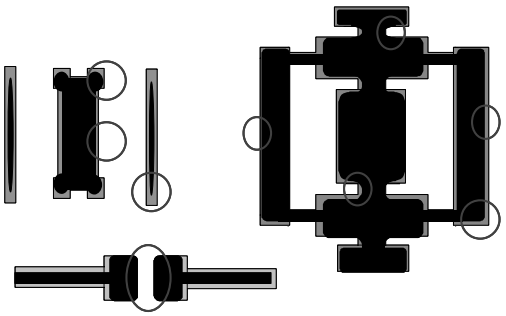

Fig. 4. An exaggerated artist rendition of the features shown in Fig. 3. The small circles highlight the types of discrepancies observed with XPA-77.

2.3 Inspection Issues with SRAFs

Sub Resolution Assist Features (SRAFs) are becoming more common in the industry. They are widely used for 90nm node wafer lithography. From a wafer lithography perspective, SRAFs are secondary features because they are not intended to print onto the wafer. They are hard to pattern accurately due to mask lithography exposure and process limitations. They often exhibit severe resolution, uniformity and or linearity issues. These issues often make high sensitivity inspection impossible because the inspection system detects these defects on SRAFs. However, SRAFs

have low wafer lithography significance[3] and do not have to be perfect. There are reticles with defects on SRAFs that are usable for wafer lithography purposes. The same types of defects, if located on primary features, would render the reticle unusable. It is necessary to inspect primary features at high sensitivity, while inspecting SRAFs at lower sensitivity. Therefore, one way to achieve this in one inspection is by implementing a method that is able to separate SRAFs from other features in real time and that applies a more tolerant defect detection sensitivity setting for SRAFs while inspecting primary features at normal full sensitivity.

3. XPE-87 DIE-TO-DATABASE INSPECTION ALGORITHM

XPE-87 is the die-to-database algorithm for high-resolution pattern inspection of reticles belonging to the 90nm node. Based on the previous XPA-77[1] TeraStar die-to-database algorithm (TeraStar SLF77 working with the XPA algorithm), XPE-87 has several enhancements that make it capable of handling the 90nm node inspection needs. As a result, XPE-87 shows a substantial performance improvement for half-tone 193nm EPSM plates. The improvement is reflected in both sensitivity and inspectability. Plates that were not possible to inspect with previous die-to-database algorithms are now inspected with XPE-87 at a high sensitivity setting. The section that follows describes the main enhancements that make XPE-87 a superior algorithm.

4. MEETING THE 90NM INSPECTION CHALLENGES

4.1 New Hardware and Software for Illumination High Gain

The XPE-87 has a new set of high gain high offset image calibration hardware that compensates for the small clear to dark illumination contrast at inspection wavelength on 193nm ArF half-tone EPSM reticles. This, together with improved software, gives the XPE-87 enough signal to perform high sensitivity inspections of ArF plates for the 90nm node. With these enhancements, the system is capable of inspecting plates made of materials that have up to 60% transmission (at the UV inspection wavelength) on the opaque area.

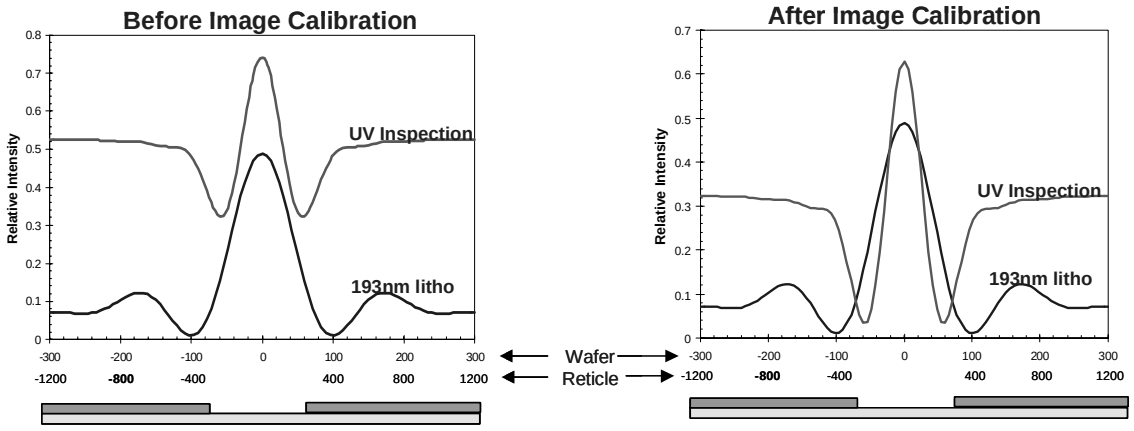

Fig. 5a. Aerial image of 193nmand UV light profiles for a 100nm clear space on ArF half-tone. Notice the UV low contrast between clear and dark intensity peaks.

Fig. 5b. Aerial image of 193nmand UV light profiles for a 100nm clear space on ArF half-tone. Notice the high contrast obtained for the UV light profile due to the XPE-87 high gain hardware and software.

Fig. 5-a shows a light profile comparison between an aerial image at 193nm and at the UV inspection wavelength for a clear space on a typical 6% transmissive half-tone ArF EPSM reticle. As described before, the light profile curve at inspection wavelength shows low contrast. Fig. 5-b shows the same comparison after image calibration is done using the XPE-87 enhanced high-gain hardware and software. Clearly, there is an increased signal that is proper for high sensitivity inspection.

To expand the concept of how a high resolution UV inspection tool with enhanced light signal gain detects defects on a 193nm ArF half-tone plate, simulations of the impact of reticle defects on a wafer were performed using PROLITH version 7.2.2. The simulations were done for both a wafer print at 193nm and UV inspection. Fig. 6 shows the wafer print intensity profiles at 193nm for a 400nm clear line (100nm on wafer) in a dark field on a 193nm half-tone reticle. Included are light profiles for a defect free case, a 100nm defect (25nm on wafer, 1/4 of linewidth) and a 140nm defect (35nm on wafer). The 140nm defect was included because it would cause a CD reduction of 10% on the wafer, certainly a defect that has to be detected. It can be observed that due to the presence of defects, there is an intensity change at the peak of the curves (the larger the defect the lower the peak). However, the location of the defect between the lines does not change the intensity curve significantly. The horizontal dashed line shows the 30% threshold typically used to simulate the clipping of a high contrast wafer resist. Therefore, the width of the aerial image at 0.3 is often used as an adequate prediction of the final wafer CD. At that level (see region inside the circle), there is a very small difference between the "no defect" curve and the ones that correspond to the section with defects. With that small difference, it is not easy to detect the defect. In fact, differences of that magnitude are common between rendered images and images on the reticle even when using the best rendering models. An extraordinarily better rendering model would be needed. Fig. 7 shows the same type of data as Fig. 6, this time for the UV inspection wavelength case. It is clear that the presence and location of the defect can be distinguished by the shift in the illumination profile and by the large area that is enclosed in between the "no defect" profile and the profile for regions with defects. The region inside the circle clearly illustrates that. Obviously, under these conditions, it is much easier for the high resolution UV system to detect the defects.

4.2 Improved Reference Data Rendering

With XPE-87, the database images that are used for comparison purposes during inspection are now rendered using an improved rendering model that considers the non-linear bias and rounding on the plate. As a result, the difference between rendered images (generated from the design data) and optical images (collected from the reticle) is minimized. This result reduces the risk of detecting false defects, allowing the inspection system to inspect at higher sensitivity settings.

In order to calculate the rendering compensation, Pre-Swath Calibration (PSC) is performed before inspection. The purpose of PSC is to find the parameters to correctly model the reference data so that it looks more like the optical image of the plate. During PSC, regions on the plate are compared to the corresponding regions on the reference data. By comparing design data to images on the reticle, manufacturing induced changes like non-linear bias and rounding, are calculated. The PSC results are then used during inspection in real time to render the database image. The PSC method that is part of XPE-87 captures and computes the information necessary for appropriate rendering, producing superior results.

Fig. 8 and 9 show a data rendering comparison between the XPA-77 and the new XPE-87. Fig. 8-a shows the image of a region on an ArF plate. Fig. 8-b shows the corresponding XPA-77 rendered database image. It is easy to notice some differences between these two images. By subtracting the rendered image from the reticle image, the XPA-77 difference image (called residues), which is displayed in Fig. 8-c, is obtained. The larger the residues, the more risk for false defect detections. Figs. 9-a, 9-b and 9-c show the same set of images for the XPE-87 case. The XPE-87 rendered image is better than the XPA-77 rendered image because it looks more like the reticle image. As a consequence, the XPE-87 residues are not as large as the XPA-77 ones. Having smaller residues, allows the tool to inspect at higher sensitivity with a low false defect count.

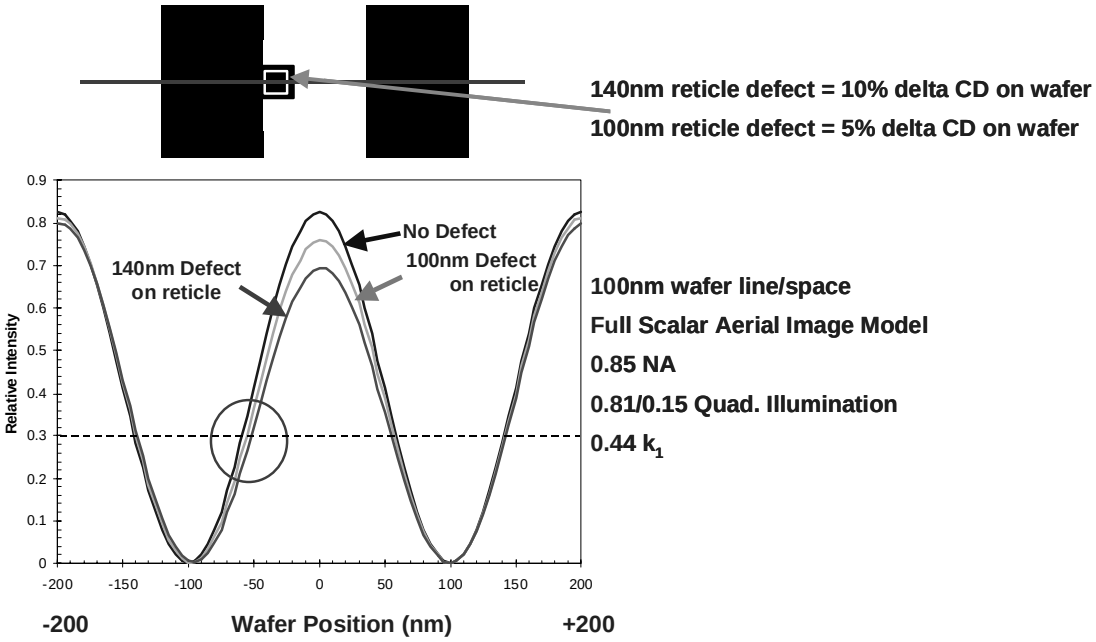

Fig. 6. 193nm wafer print simulation for defects on a clear space on a 193nm half-tone reticle. The separation between the "no defect" curve and the curves corresponding to defects around the 30% intensity is small (5% for the 100nm reticle defect and 10% for the 140nm reticle defect).

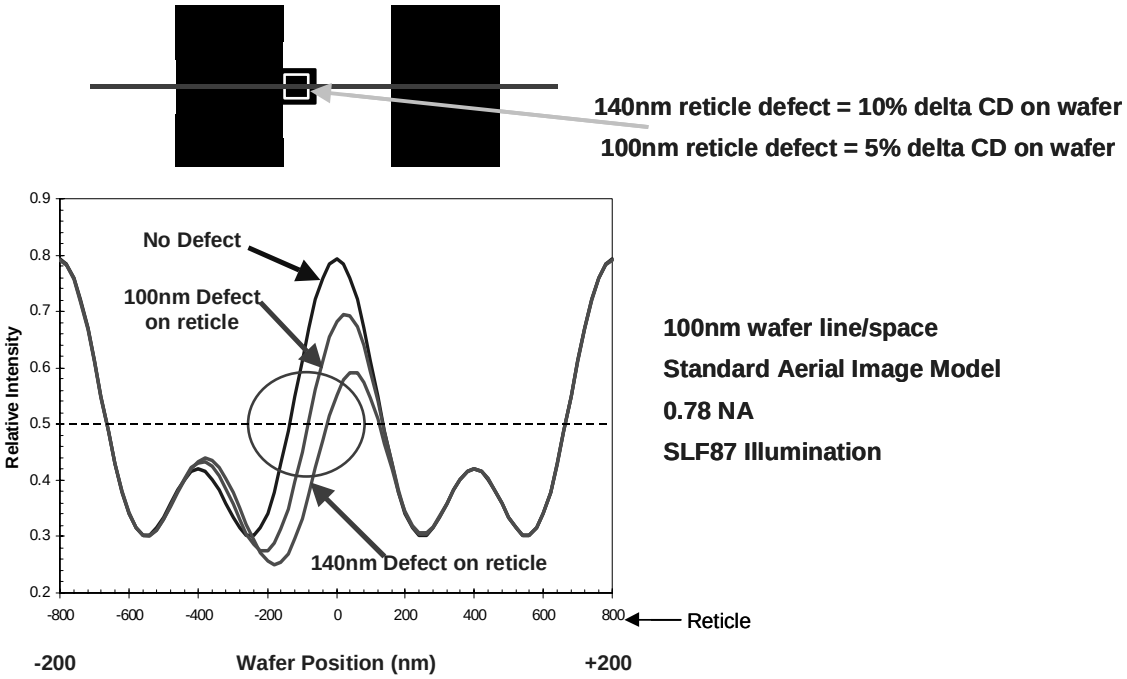

Fig. 7. UV reticle inspection simulation for defects on a clear space on a 193nm half-tone reticle. The difference between the "no defect" curve and the curves corresponding to defects is substantial. Under these conditions, it is easier for an inspection system to detect the defects.

A practical application of how smaller residues improve the chances for high sensitivity inspection is shown in Fig. 10, where a small region of a plate that had a very large false defect count when inspecting with XPA-77 is shown. The center image was captured from the plate during inspection. The picture on the left shows the corresponding XPA-77 rendered image. Because of residues, XPA-77 detected a false defect inside the displayed region. The image on the right shows the residues from XPE-87. They are smaller than the XPA-77 residues. As a consequence, the false defects are eliminated, allowing the XPE-87 to inspect with high defect detection sensitivity.

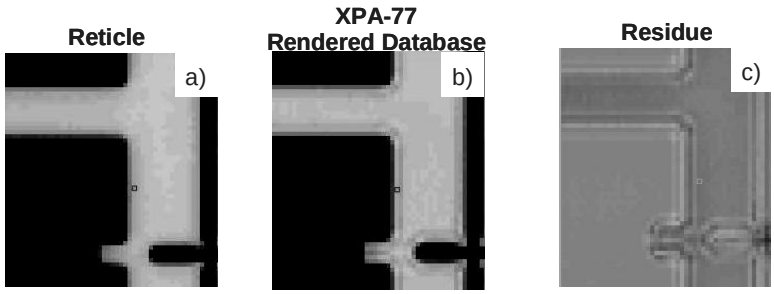

Fig. 8. Sample region showing the reticle image, the corresponding XPA-77 rendered image and the XPA-77 residues image (residues are obtained by subtracting the database image from the reticle image). XPA-77 residues are large enough to cause false defect issues when inspecting 90nm plates at high sensitivity.

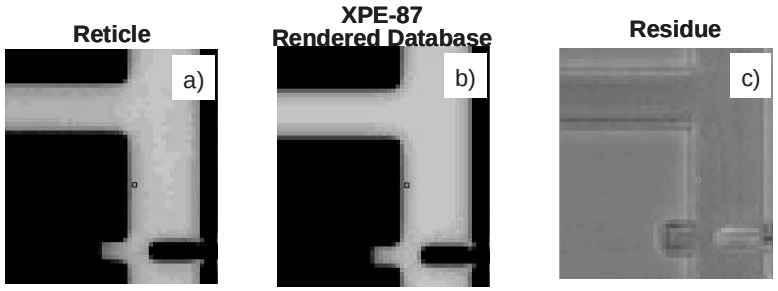

Fig. 9. Sample region showing the reticle image, the corresponding XPE-87 rendered image and the XPE-87 residues image (residues are obtained by subtracting the database image from the reticle image). Because XPE-87 has smaller residues than XPA-77, it can inspect the reticle at higher sensitivity.

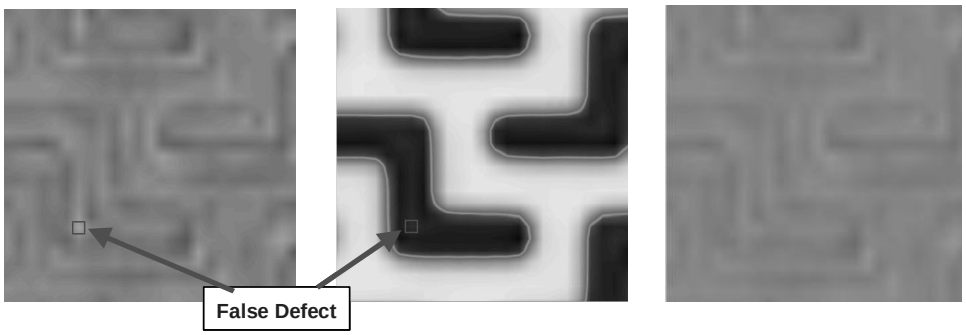

Fig. 10. A practical comparison of the effect of rendered images on inspection results. The comparison is between XPA-77 (left image) and XPE-87 (right image) for the plate region shown in the center image. Because of higher residues, XPA-77 detects false defects. XPE-87's image shows smaller residues, eliminating the false defects.

4.3 AssistSmart™ Independent Sensitivity Threshold for SRAFs:

It is common to see assist lines on 193nm EPSM reticles that do not have the same process linearity and or uniformity as the main pattern. This could cause a high defect detection count, which in turn, may make the plate un-inspectable unless the inspection is desensitized. Often, the defects detected on assist lines are not considered important and need to be discarded (also know as nuisance defects). Globally desensitizing the inspection is not an ideal solution, since the main patterns still require a high sensitivity inspection. The XPE-87 AssistSmart tool presents a better solution. AssistSmart detects assist lines in the inspection region, allowing the user to reduce the sensitivity for assist lines when needed while still maintaining a high sensitivity setting for main pattern. The benefits that AssistSmart provide were obvious during the XPE-SLF87 alpha and beta tests. Critical EPSM 90nm node reticles for several layers were inspected with high sensitivity for primary features and lowered sensitivity for defects on SRAFs (refer to section 6 for a XPE-87 and XPA-77 results comparison example). These plates were not considered "inspectable" with XPA-77 due to the large number of defects detected on SRAFs.

5. XPE-87 PERFORMANCE ON PROGRAMMED DEFECT PLATES

XPE-87 has been characterized using the Spica-400 193nm EPSM test plate. Spica is a programmed defect test plate designed for characterization of 90nm node inspection algorithms. It is manufactured using 50 KeV writing tools. Based on SEMI Standards P22 and P23 (SEMI draft document 2810), Spica has a collection of defects programmed over geometry that is representative of common features on production plates (to identify the defect types included in Spica see the top of Fig. 11). Most of the characterization tests were done using an ArF version of Spica. Tests were also done using KrF and COG versions.

A sensitivity comparison between XPA-77 and XPE-87 was performed. Initially, a production 90nm ArF plate with SRAFs was inspected with both XPE-87 and XPA-77. XPE-87 was able to inspect the production plate at high sensitivity without the false defects problem. XPA-77 however, detected too many nuisance/false defects. Because of that problem, XPA-77 was desensitized in order to make the inspection possible. The XPE-87 and XPA-77 sensitivity settings used for the production plate were then used for the inspection of Spica. Fig. 11 shows a sensitivity chart that includes the detection lines for XPE-87 and XPA-77 plus the nominal XPE-87 specification. On this chart, all defects that are located under the detection line were detected at a 100% rate. Looking at the chart, it is clear that XPE-87 outperforms XPA-77 by a wide margin (the XPE-87 detection line is above the XPA-77 one indicating that XPE-87 detected more defects at a 100% rate). XPE-87 also meets or exceeds its nominal specification (100nm for edge defects and 80nm for CD defects). The Spica XPE-87 results were obtained with a very low false defect count (XPA-77 detected around 60 false/nuisance defects per inspection).

6. XPE-87 RESULTS ON PRODUCTION PLATES

A large sample of plates from several manufacturers has been inspected with XPE-87. Included were ArF, KrF and COG plates. Most of the efforts were concentrated on inspecting ArF plates for the 90nm node, especially plates with challenging designs and SRAFs. Also, when possible, a comparison was performed for inspections done with XPE-87 and XPA-77 (some of the plates are not inspectable with XPA-77). The performance improvement for 90nm node EPSM reticles with SRAFs is significant. Plates that were not considered "inspectable" with the XPA-77 were inspected with XPE-87 at high sensitivity. For COG plates, the performance of XPE-87 is similar to the performance of XPA-77.

Fig. 12 shows a comparison of inspections of the same 90nm EPSM production plate (with SRAFs) when inspecting it with XPA-77 and XPE-87. When inspecting with XPA-77, the inspection system was able to handle only few swaths due to the very large number of false defects (or real defects on SRAFs that are not lithographically significant). Obviously, this plate is not inspectable with XPA-77. The same plate was then inspected with XPE-87 at a high sensitivity setting for primary features (using SmartAssist to filter out small defects on SRAFs). XPE-87 was able to inspect the plate without problems detecting more than 300 defects (all real defects, some of them very small). Fig. 12 shows the inspection maps for the XPA-77 and XPE-87 inspections.

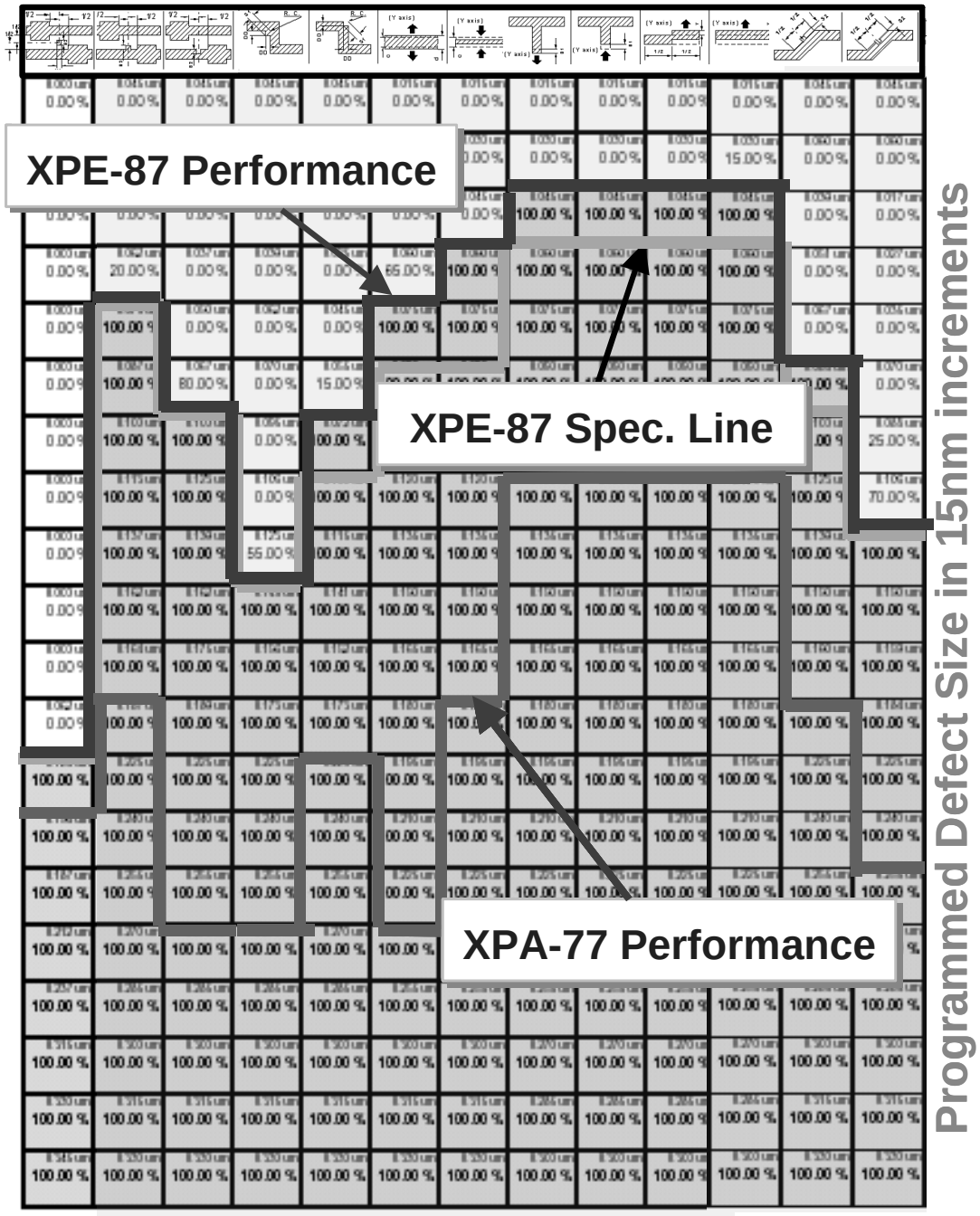

Fig. 11. Sensitivity chart showing the results for XPE-87, XPA-77 and the nominal XPE-87 specification. The Spica ArF 193nm test reticle was used for the tests. Defects below the sensitivity performance line were detected at a 100% rate. Sensitivity settings used for production 193nm half-tone reticles were used to collect the results. XPE-87 shows significant performance improvement over XPA-77. Twenty inspections were analyzed. For each inspection XPE-87 false defect count was very low or zero. XPA-77 detected an average of 60 false defects.

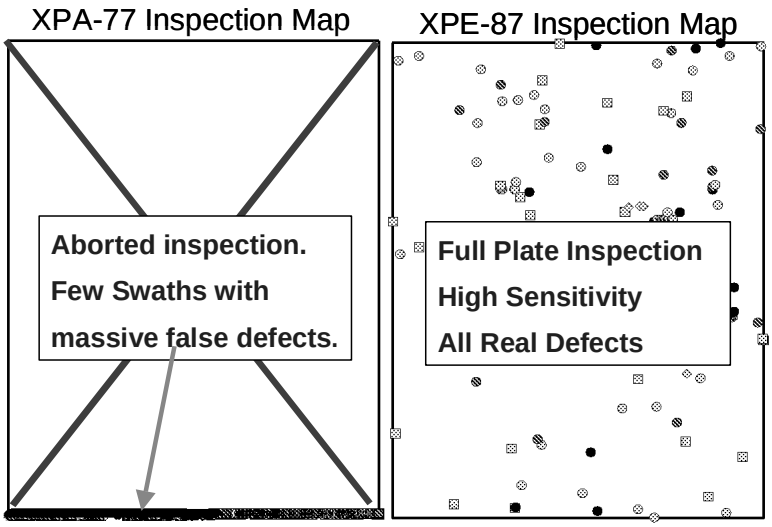

Fig. 12. XPA-77 vs. XPE-87 inspection maps of the same ArF 193nm half-tone plate with SRAFs. XPA-77 was unable to inspect the plate, aborting the inspection due to a very high false defect count. XPE-87 inspected the full plate at high sensitivity without false defects.

7. CONCLUSIONS

Before the developments described in this paper, die-to-database inspection tools were unable to meet the inspection requirements of ArF 193nm half-tone reticles for the 90nm node. ArF high transmission at inspection wavelength, 2-D non-linearity and issues with SRAFs were the main roadblock for inspection.

XPE-87, a new die-to-database inspection algorithm meets the ArF half-tone 90nm node inspection requirements with high sensitivity, low false defect count on full field plates.

- XPE-87's low residue 2-D non-linear model, new software and hardware for high illumination gain and AssistSmart feature make the XPE-87 capable of meeting the 90nm node inspection requirements.

ACKNOWLEDGEMENTS

The authors want to acknowledge the work of the KLA-Tencor Engineering and Applications teams.

REFERENCES

(1) William W. Volk, et al, "Multi-Beam High Resolution Die-to-Database Reticle Inspection", 21st Annual Bacus Symposium on Photomask Technology, Giang T. Dao, Brian J. Grenon, Editors, Proceedings of SPIE Vol. 4562, p. 111-121 (2002).

(2) Chris A. Mack, "Electron Beam Lithography Simulation for Mask Making, Part III: Effect of Spot Size, Address Grid and Raster Writing Strategies on Lithography Performance with PBS and Zep-7000" 18th Annual Bacus Symposium on Photomask Technology, Brian J. Grenon, Frank Abboud, Editors, Proceedings of SPIE Vol. 3546, p. 32-44 (1998).

(3) Adam Konstantinos, et al, "Analysis of OPC features in binary masks at 193nm", Optical Microlithography XIII, Christopher J. Progler, Editor, Proceedings of SPIE Vol. 4000, p. 711-722 (2000).